Supporting Information

"Molecular Threading" and tunable molecular recognition on DNA origami nanostructures

Na Wu[†], Daniel M. Czajkowsky[‡], Jinjin Zhang[†], Jianxun Qu[‡], Ming Ye[†], Dongdong Zeng[†], Xingfei Zhou[#], Jun Hu[*,†], Zhifeng Shao[‡], Bin Li[*,†], Chunhai Fan[*,†]

[†] Division of Physical Biology, and Bioimaging Center, Shanghai Synchrotron Radiation Facility, Shanghai Institute of Applied Physics, Chinese Academy of Sciences, Shanghai 201800, China. [‡]School of Biomedical Engineering, Shanghai Jiao Tong University, Shanghai 200240, China. [#]Physics Department, Ningbo University, Ningbo Zhejiang 315211, China.

Experimental Section

Molecular Dynamics Simulations and Analysis. The 4-strand B-DNA assembly, where the strands were either all adenine or all thymine, was first constructed as depicted in Figure 1. The ends of the DNA strands at the boundary of this assembly were linked to their periodic image in the neighboring unit cell, thereby forming effectively an infinite origami block. The system was then solvated in TIP3 water,[1] ionized to 20mM $MgCl_2$, and then minimized and equilibrated using VMD/NAMD[2,3] and the CHARMM 27 force field,[4] in the constant-pressure and constant-temperature

(NPT, 295K, 1atm) ensemble. Similar results were obtained at 12.5mM $MgCl_2$.

Periodic boundary conditions were applied in all spatial directions. The temperature and pressure were controlled by the Berendsen thermostat and barostate with a coupling time of 0.1ps and 1.0ps, respectively. The particle mesh Ewald algorithm was employed to treat electrostatic interactions. The van der Waals interactions were treated with a cut-off of 12Å, and the integration step was set to 2fs. After ~1ns, the system achieved an equilibrated configuration, as judged by the root-mean-square deviation of the DNA backbone. It should be noted that, owing to the difference between the 10.67bp/turn feature of this rectangular origami sheet and the preference of B-DNA for 10.4bp/turn, a global twist of the 2D sheet is expected[5]. Indeed, at the end of these simulations, the structure was slightly deformed (Figure S1). However, the extent of this deformation in these simulations was probably constrained owing to the periodic boundary conditions. For the measurement of the hole size, the smallest distance between phosphate oxygen atoms on opposing DNA strands bordering a hole was determined every 10ps along the trajectory. This corresponds to a measurement of the hole size along the **b**-direction roughly every 1.5nm.
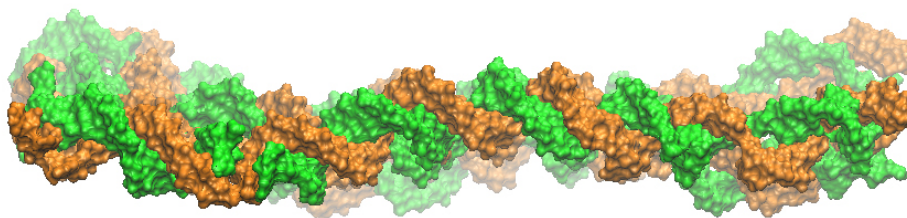

Figure S1. Slight deformation of the simulated 2D origami sheet.

The ABF simulations[6,7] derived for the NVT ensemble in NAMD, were employed to determine the potential of mean force associated with the translocation of a 5-dT ssDNA molecule through a hole in the origami sheet. A restraining harmonic potential was applied to two of the phosphates of the 5-dT molecule to constrain the motion along the reaction coordinate, the distance through the center of a hole in the origami in the plane of the 2D sheet (Figure S2). The simulations were performed in two stages. In the first, the entire reaction coordinate was partitioned into 1.5Å, partially overlapping, segments, and the ABF simulations were performed in each of segment. Only after the simulations were performed long enough to observe convergence (diffusive motion and an even distribution of sampling across the reaction coordinate) within one segment were simulations initiated in an adjoining, partially overlapping region. In the second stage, the resulting PMF profile of each of these segments was combined into larger 5Å segments, and the simulations were performed over these larger segments to verify an absence of any influence of the segmentation method employed on the resulting PMF profile. Again, in this second stage, simulations were performed long enough to observe convergence of the system. The results from these 5Å segments were then combined to produce the final PMF profile (Figure S2).
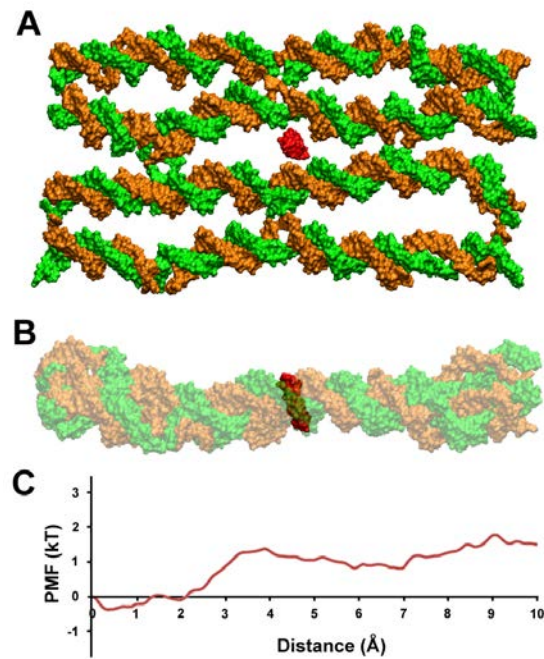
Figure S2. Free energy (PMF), determined from ABF simulations, associated with a threading ssDNA molecule through the 2D origami. (A) Top-view of the system with the 5-dT ssDNA (red) in mid-translocation through the 2D origami (green and orange). (B) Side-view of the system, with the origami partially transparent. (C) Translocation of the ssDNA through the hole is associated with energetic barriers of less than 2kT in height, which can be easily overcome with thermal fluctuations.

Sample preparation. The DNA origami experiments were performed as previously described.[8,9] Briefly, the template single-stranded M13mp18DNA (New England Biolabs) and the 216 short oligonucleotides 'staple strands' (Sangon Biotech Co., Ltd, Shanghai) were incubated together at a mol ratio of 1:10 in $1\times$TAE/Mg^{2+} buffer (40mMTris, 20mM Acetate, 2mM EDTA, 12.5mM Mg^{2+}, pH 8.0). The sample was annealed from 95ºC to 25ºC at a rate of 0.1ºC/10s in a PCR instrument (Eppendorf Mastercycler Personal Machine). With all biotinylated staple strands, the biotin

moiety, with or without spacers (poly-thymidine, dT), was attached to the 5'-end of the staple strand.

AFM imaging and analysis. Time-lapse AFM experiments were performed as previously described.[9] Briefly, a drop of 2μl biotin-modified DNA origami was placed on a freshly cleaved mica surface and incubated for several minutes. After this, 30μl of the TAE/Mg^{2+} buffer was then added to the sample, and then it was imaged by AFM. During imaging, a 30μl drop of SA (Sigma-Aldrich. St. Louis) in 1×TAE/Mg^{2+} was slowly injected to a final concentration of 7.6nM. Continuous *in situ* tapping mode images were then acquired (for up to 50min), applying a minimal force to reduce tip-sample interactions. The original images were sampled at the resolution of 256×256 points and the scan rate was 2Hz. All the images were obtained using a Nanoscope IIIa-Multimode AFM (Veeco-Digital Instruments, Santa Barbara, CA) with a J scanner, and NP-S silicon nitride probes with a nominal spring constant of 0.58N/m (Veeco). The images were collected and flattened for later data analysis. Binding efficiency was defined as the ratio of the number of observed SA bound to the total number of biotin ligands on each origami (four).

For FM-AFM imaging, the sample preparation was the same as with the time-lapse AFM mentioned above. Imaging was performed using our home-made FM-AFM (Nanosurf EasyPLL plus detector and Veeco Nanoscope 3D sample controller). The images were obtained under solution using NSC15 tips (MikroMash, USA) with a spring constant of 42N/m at a resonance of about 160kHz, scanning rate

of 7Hz, oscillation amplitude of 0.35nm, and frequency shift of 35Hz. With FM-AFM, the cantilever is driven into resonance and the shift in the frequency that occurs when the tip interacts with the sample is measured and maintained at a constant value during imaging.[10-12]
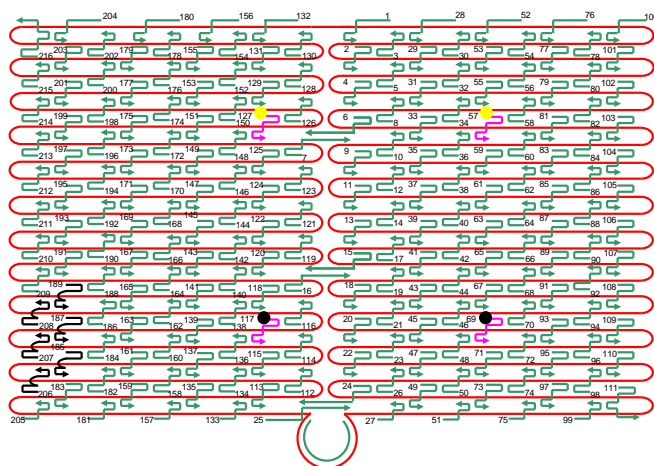

Figure S3. Schematic illustration of the origami used in the time-lapse experiments shown in Figure S4 (below). The black spheres reflect locations without any ssDNA spacer (0-dT) and the yellow spheres reflect locations with 5-dT spacers. The black staple strands (bottom left corner) depict the locations of additional poly-dT segments that enable identification of the origami orientation on mica.
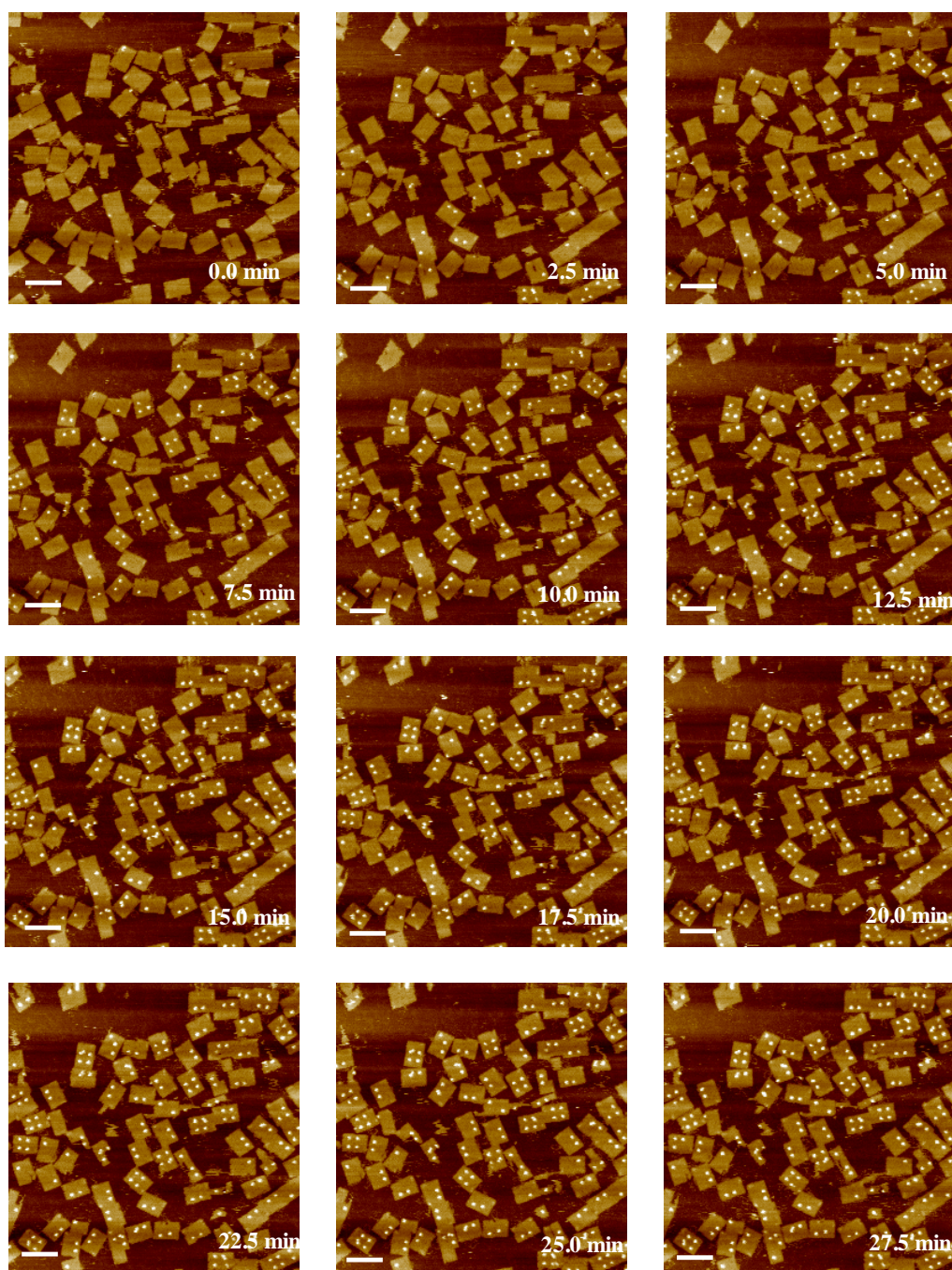
Figure S4. Time evolution of the SA-binding process to 2D origami depicted in Figure S3 (Scale
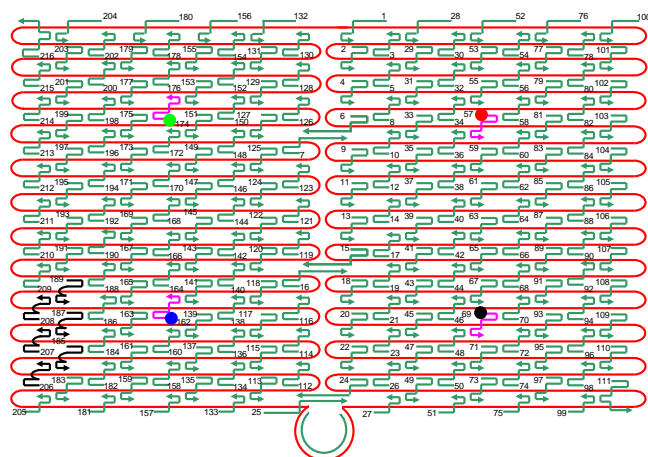
bar:150 nm).

Figure S5. Schematic illustration of the origami used in the longer-spacer (15-dT and 20-dT) experiments. The colored spheres depict the locations of the spacers with a length of 5-dT (black), 10-dT (red), 15-dT (blue), and 20-dT (green).
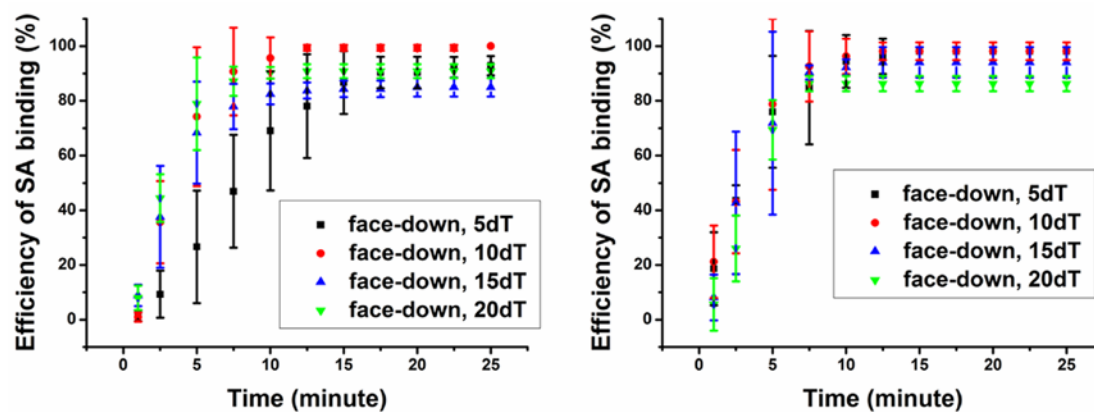

Figure S6. SA-binding dynamics as a function of different spacer lengths.

References

(1) Jorgensen, W. L.; Chandrasekhar, J.; Madura, J. D.; Impey, R. W.; Klein, M. L. *J. Chem. Phys.* **1983**, *79*, 926.

(2) Humphrey, W.; Dalke, A.; Schulten, K. *J. Mol. Graph.* **1996**, *14*, 33.

(3) Phillips, J. C.; Braun, R.; Wang, W.; Gumbart, J.; Tajkhorshid, E.; Villa, E.; Chipot, C.; Skeel, R. D.; Kale, L.; Schulten, K. *J. Comput. Chem.* **2005**, *26*, 1781.

(4) MacKerell Jr, A. D.; Bashford, D.; Bellott, M.; Dunbrack Jr, R. L.; Evanseck, J.; Field, M.; Fischer, S.; Gao, J.; Guo, H.; Ha, S. *J. Phys. Chem. B* **1998**, *102*, 3586.

(5) Woo, S.; Rothemund, P.W.K. *Nat. Chem.* **2011**, *3*, 620.

(6) Darve, E.; Wilson, M. A.; Pohorille, A. *Mol. Simulat.* **2002**, *28*, 113.

(7) Rodriguez-Gomez, D.; Darve, E.; Pohorille, A. *J. Chem. Phys.* **2004**, *120*, 3563.

(8) Ke, Y. G.; Lindsay, S.; Chang, Y.; Liu, Y.; Yan, H. *Science* **2008**, *319*, 180.

(9) Wu, N.; Zhou, X. F.; Czajkowsky, D. M.; Ye, M.; Zeng, D. D.; Fu, Y. M.; Fan, C. H.; Hu, J.; Li, B. *Nanoscale* **2011**, *3*, 2481.

(10) Sheikh, K. H.; Jarvis, S. P. *J. Am. Chem. Soc.* **2011**, *133*, 18296.

(11) Asakawa, H.; Yoshioka, S.; Nishimura, K.-i.; Fukuma, T. *Acs Nano* **2012**, *6*, 9013.

(12) Ido, S.; Kimura, K.; Oyabu, N.; Kobayashi, K.; Tsukada, M.; Matsushige, K.; Yamada, H. *ACS Nano* **2013**, *7*, 1817.